A Highly Integrated Dual Band SiGe BiCMOS Power Amplifier that Simplifies Dual-band WLAN and MIMO Front-End Circuit Designs

Chun-Wen Paul Huang, Mark Doherty, Philip Antognetti, Lui (Ray) Lam, and William Vaillancourt

SiGe Semiconductor, 200 Brickstone Square, Suite 203, Andover, MA 01810, USA

***Abstract* — A highly integrated SiGe BiCMOS power amplifier for dual-band WLAN applications is presented. The PA has 2 and 3 stages of amplification for the 'b/g' and 'a' band, respectively, and integrates the input/output matching network, out-of-band rejection filter, power detector, and bias control. The die area is 1.7 x 1.6 mm^2. The b/g amplifier achieves 28 dB gain with 19.5 dBm output power at 3% EVM and 185mA and harmonics of <-45dBm/Mhz. The a-band amplifier achieves 30 dB gain with 3% EVM at 19.0 dBm output with 220mA of current and harmonics < -50 dBm/MHz. The reported PA linearity, out-of-band rejection, and integration level exceeds previously reported WLAN dual-band SiGe PA designs.**

***Index Terms* — WLAN power amplifier, dual-band PA, dual-band front-end module.**

I. Introduction

Wireless LAN (WLAN) radio applications have extended beyond traditional computer networking to many other electronic appliances, such as cellular phones, PDA, electronic gaming devices, security and monitoring systems, and multi-media systems [1]. A natural evolution of this technology is the use of multiple-input, multiple-output (MIMO) technique to increase the data rate from the 54 Mbps to a minimum of 108 Mbps. Most WiFi and MIMO radios operate at 2.4 GHz with a band that has 3 channels for 54Mbps operation. For MIMO applications, the channel bonding technique is widely applied. Therefore, dual-band WLAN and MIMO will be increasingly adopted to avoid future bandwidth congestion. The embedded WLAN radios in portable electronic devices usually require more compact and integrated designs than a WLAN radio used in computer networking applications. Moreover, a front-end module (FEM) is often the preferred design implementation. Specifically in cases where MIMO is used in portable electronics, FEM's simplify the design and layout of a compact radio and reduces BOM count in a multichannel MIMO configuration. To simplify a dual-band FEM design, single or 2 to 3 chip integrated IC designs will be a future trend for size, yield, and cost considerations.

In this paper, a highly integrated WLAN dual-band power amplifier is presented. As shown in Fig. 1, the PA design is based on SiGe BiCMOS technology using through-silicon via with a die size of 1.7 x 1.6 mm^2. The PA integrates input and output matching network, out-of-band spur rejection filter, harmonic rejection filter, voltage regulator and bias circuits, temperature-compensated power detector, and CMOS compatible enable circuitry. In addition to the integration, the dual-band PA also demonstrates unparalleled RF performance, exceeding previously published designs [2-4]. Both low and high band amplifiers are controlled by the on-chip temperature and voltage compensated bias control. For 2.4 to 2.5 GHz, the b/g band PA delivers 28 dB gain and 19.5 dBm linear power at 54Mbps with EVM < 3% and total current consumption <185 mA. For 4.9 to 5.9 GHz, the a-band PA delivers 29 dB gain and > 19 dBm at 54 Mbps with EVM < 3% and total current consumption <220 mA.

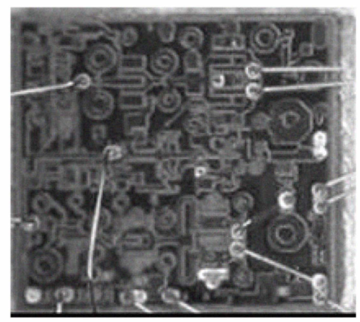

Fig. 1. Die photo of the dual-band WLAN amplifier based on SiGe BiCMOS technology.

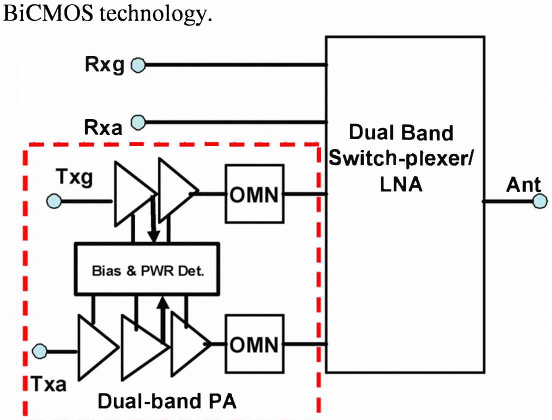

Fig.2. A novel dual-band WLAN FEM architecture for WLAN a/b/g/n radios.

The power detector is designed to be insensitive to power supply voltage, temperature, and antenna load mismatch up to 3:1 VSWR with variation within 0.5-1.0 dB. The on-chip rejection filters suppress the VCO spurs at 1.6 and 3.2 GHz for b/g band PA and the spurs at 3.8 and 7.2 GHz for a-band PA. In addition, the harmonic rejection filters are also integrated in each PA's output matching networks, which ensures harmonic emission < -45 dBm/MHz up to the maximum linear output power without the need of any external filtering. All these unique features simplify the front-end design of 802.11 a/b/g WLAN radio. With a dual-band switch-plexer or switch with integrated LNA [5], a complex dual-band front-end module can be constructed with two integrated circuit building blocks: a dual-band power amplifier and a dual-band switch-plexer or switch LNA.

II. Design

The power amplifier design will be presented in 2 subsections: (A) Technology, (B) Topology.

A. Technology

SiGe BiCMOS is a proven technology for b/g PA design [5]. However, several major challenges were found in realizing an amplifier with high gain and linearity at 6 GHz in silicon. Fundamentally, increasing linear output power at high frequency with acceptable efficiency trends inversely proportional to the lithography node due to breakdown challenges and associated CMOS device linearity. Si and SiGe bipolar devices tend to trade-off breakdown voltage for improved unity-gain cut-off frequency. Starting with a self aligned SiGe process, a new epitaxial layer profile had to be developed to move to higher "f_T x BVceo" product resulting in improved gain/power performance at high frequency with f_T of 37 GHz at a Vcb = 0V and BVceo of 6V.

Another well known challenge for an 'a'-band PA is achieving the required gain concurrently with gain flatness across the frequency band. To achieve the necessary power gain, through-silicon-via (TSV) were incorporated into the technology to reduce impedance to ground on the emitters without resorting to numerous ground bond wires. Prior to finalizing the design, a custom design flow with extensive electromagnetic modeling was developed to improve the ability to handle large simulation problems and capture all proximity effects in the silicon substrate.

Not surprisingly, using a BiCMOS technology platform greatly enhances the opportunities for integration in the context of advanced RF components. The design leverages BiCMOS to incorporate the PA bias' band-gap reference, enable/pull-down switch, and temperature compensated power detectors. For portable electronic devices, current consumption is a key parameter in system design. Moreover, accurate power detection can enhance the effective transmitted power by reducing power control errors and guaranteeing regulatory compliance.

B. Topology

As shown in Fig. 2, the dual-band PA consists of a 2 stage amplifier for 'b/g' band and a 3-stage amplifier for 'a'-band. The major consideration for using a 2 stage b/g band PA is that transmitter radios today can deliver greater linear input power, relieving the dependence on high gain from the b/g band PA. In this design, both PA's are controlled by an integrated control block providing reference current for current mirrors and on/off control.

During WLAN communications, the PA is frequently enabled and disabled to reduce current consumption. Typically, GaAs PA's often suffer in dynamic mode operation due to the poor thermal characteristics of the GaAs substrate. Moreover, GaAs designs often need external speed-up circuits to improve dynamic mode linearity. The PA design herein employs an advanced topology to mitigate the thermal difference between PA stages, which results in no degradation in both linearity and gain under dynamic mode operations.

An accurate power detector may require a directional coupler to isolate and reduce the impact from reflected signals. Instead of using a directional coupler, this design uses a novel approach [6] to buffer the detector from these effects. The power detector is realized within the inter-stage matching circuit between driver and output stage. When the last inter-stage matching network is appropriately designed, the gain flatness is naturally ensured. In addition, the power detection based on signal coupling at the inter-stage matching network will produce a uniform output voltage response across the entire bandwidth. The isolation from the 3rd stage device and the last inter-stage matching network provides sufficient isolation, effectively acting as an active directional coupler.

To illustrate the PA topology, the 3-stage 'a'-band PA is shown in Fig. 3. Perhaps the most challenging part of SiGe RF amplifier design is the on-chip matching. Using measurement based transistor models and large-scale electromagnetic based models can enhance the chances of having first pass design success. The out-of-band rejection filtering is well integrated in the input matching network and 1^{st} and 2^{nd} stage inter-stage matching networks. The output matching network not only provides optimal matching for in-band but also includes the harmonic termination. A typical design consideration is to use a 2^{nd} harmonic short as shown in Fig. 3 to not only enhance the linearity but also effectively short the 2^{nd} harmonic to ground.

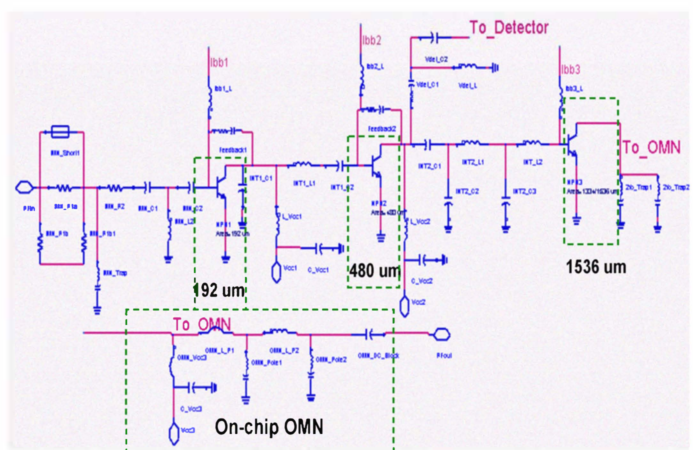

Fig. 3. Conceptual schematic of the a-band PA design.

The 3^{rd} harmonic emission is typically much lower in magnitude than the 2^{nd}. Therefore, the L-C networks of a dual-pole matching network will effectively prevent the 3rd harmonic emission.

III. PERFORMANCE

Measurements of the dual-band WLAN PA design are presented in this section. Fig. 4 shows the small signal gain of ‘b/g’ and ‘a’ band transmit paths. The gain variation is within 0.5 dB for ‘b/g’ band and 1.0 dB for ‘a’ band. Linearity of the dual-band PA is validated using an OFDM signal at 54 Mbps and under dynamic mode of pulsing PA enable instead of providing a constant voltage at the PA enable. As shown in Fig. 5 and Fig. 6, ‘b/g’ band transmit chain delivers > 19.5 dBm at 3% dynamic mode EVM (DEVM) with 185 mA current consumption. The ‘a’-band PA can also delivers 19-19.5 dBm at 3% DEVM with 220 mA current consumption. The PA also delivers more than 2 dB additional linear power at 4.5 V and 1.0 dB less linear power at 2.7 V.

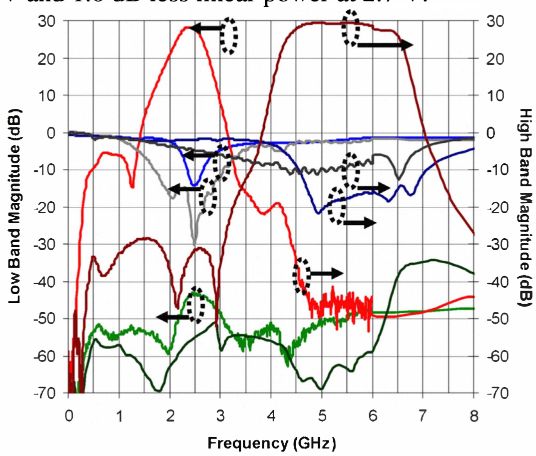

Fig. 4. Measured S-parameters of the WLAN dual-band PA.

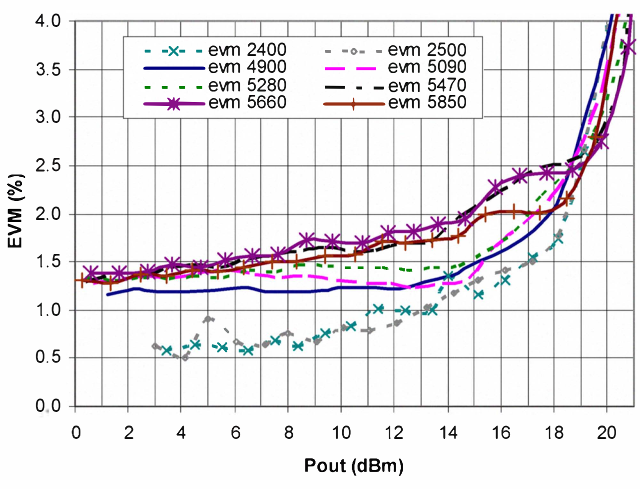

Fig. 5. Measured dynamic mode EVM at 54 Mbps of the SiGe dual-band WLAN PA.

The harmonic emissions were also validated and are shown Fig. 7. The worst cases were found at the harmonics of 21 dBm output at 1Mbps for the ‘b/g’ transmit chain and 19 dBm at 54 Mbps for the ‘a’-band transmit chain. Harmonic emission levels of most channels under test are below -50 dBm/MHz up to the maximum linear output powers. Therefore, the PA can be used in a front-end module design without using external harmonic filters. In addition, based on the FCC requirement of -41.2 dBm/MHz, the PA provides sufficient margin for the radio designs using a high gain antenna. Spurious emissions under load mismatch were also verified. The PA stability was confirmed to a VSWR 6:1 (load mismatch) while the input was overdriven to +12dBm without any spurious emissions.

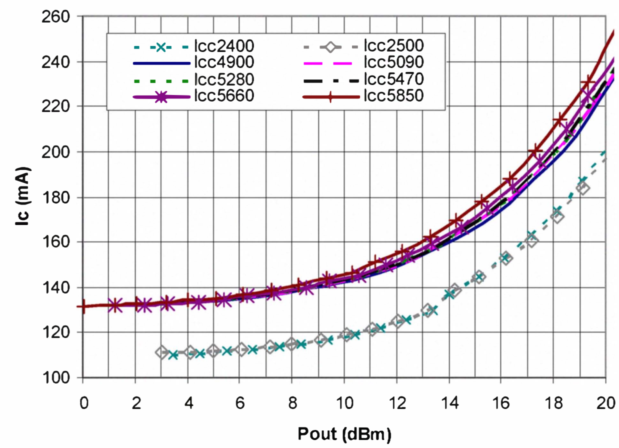

Fig. 6. Measured total current consumptions for the presented SiGe dual-band WLAN PA with a 3.3 V supply voltage.

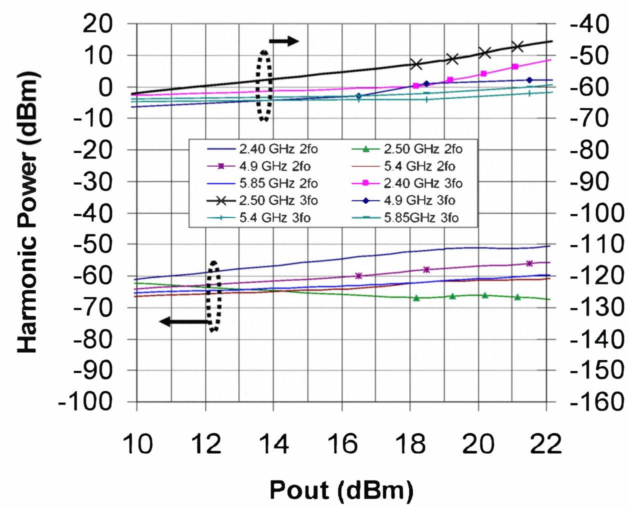

Fig. 7. Measured harmonic emission for b/g and a band PA with a 3.3 V supply voltage.

The PA performance under wide temperature variations of -10 to 85 °C was also confirmed. As shown in Table 1, excellent temperature stability and tight performance variation versus temperature are seen primarily because of the on-chip temperature compensated biasing circuitry, combined with the good thermal conduction characteristics of silicon substrate. A comparison of the PA linearity and gain variation under various temperatures and bias voltages is shown in Table 1. At the highest temperature, linear power is degraded by 1 dB, whereas at -10°C, the PA has 0.6 dB better linear gain than at room temperature. The gain variation versus temperature also follows the same trend. The linearity and gain versus +/- 10% power supply voltage were measured to be 1 and 0.3 dB, respectively.

The power detectors were also characterized under temperature variation, power supply voltage, and load mismatch. The power detector characteristic for 'a'-band PA is shown in Fig. 8. The 'b/g' band power detector has a similar characteristic to that of the 'a'-band PA. The variations for temperature and voltage were found to be 0.6 dB or +/-0.3 dB and 0.5 dB or +/- 0.25 dB, respectively. The detector variation under the load mismatch up to VSWR 3:1 was found to be within 1 dB. This level of consistency of performance can enhance the power detection accuracy over the entire linear power operating range, which can help the radio transmit maximum power while meeting FCC regulatory requirements for emission levels.

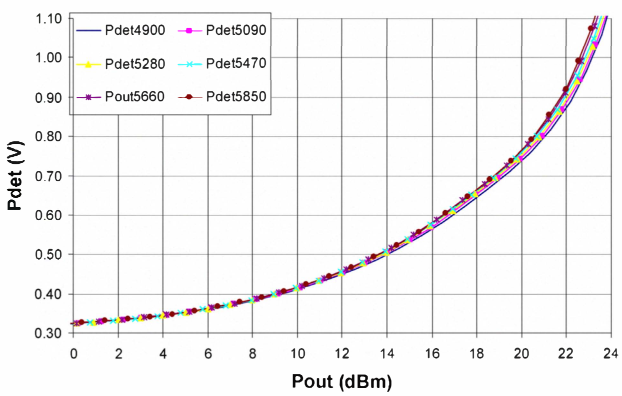

Fig. 8. Measured harmonic emission for b/g and a band PA with a 3.3 V supply voltage.

	b/g Band PA		a Band PA	
Temperature (°C)	-10	85	-10	85
Gain	0.5	-1.5	0.3	-2.5
EVM = 3%	0.2	-0.8	0.25	-1.4
1 dB Compression	0.2	-1.5	0.25	-1.2
Power Detector	0.25	-0.25	0.3	-0.3

Table 1 Performance variations (in dB) of the presented dual-band WLAN PA versus temperatures variation.

Comparing these measurements against the performance of previously published dual-band WLAN PA designs, we note that GaAs PA presented in [2] has insufficient 'a'-band bandwidth and low integration due to its dependence on external surface mount component for matching networks. In addition, SiGe PA presented in [3] and CMOS PA presented in [4] both have high EVM levels which will result in high packet error rate and requires more transmit time or current consumption. Moreover, [3] has noticeable gain slope in 'a'-band PA. These comparisons confirm the view that a highly integrated SiGe-based amplifier serving both the 'b/g' and 'a' band delivers unprecedented performance and advantages. These advantages encompass both the traditional RF figures of merit (such as dynamic linearity) and other control features that are highly useful to the system integrator in a variety of WLAN applications.

IV. Conclusions

In this paper, a 1.7 x 1.6 mm^2 SiGe BiCMOS dual-band WLAN power amplifier is presented. The PA features advanced integration complexity and functionality, which provides a turn-key solution for WLAN front-end designs. The 'b/g'-band amplifier achieves 28 dB gain with 19.5 dBm output power at 3% dynamic mode EVM with harmonics <-45 dBm/MHz, while consuming 185mA of current from a 3.3V supply. The 'a'-band amplifier achieves >29 dB gain with 3% dynamic mode EVM power of 19.0 dBm with 220 mA of current and harmonics < -50dBm/MHz. The integrated temperature and voltage compensated bias circuit ensure the minimal variation of performance under extreme temperature and supply voltage variations. The power detector is relatively insensitive to load, temperature, and supply voltage variations, which enable an accurate closed loop control within the entire linear output power operation. Based on the unparalleled RF performance and integration level, this PA can be used as a key building block that simplifies the construction of a dual-band front-end circuit designs for the existing 'a/b/g' and the fast growing MIMO 'a/b/g/n' WLAN applications. With a dual-band switch-plexer [5] or a switch with dual-band LNA, an 'a/b/g/n' FEM can be easily realized in a 2-chip design as shown in Fig. 2. In addition to the integration and functionality described, the dual-band WLAN performance was measured to surpass previously published WLAN dual-band PA designs in linearity, gain flatness, out-of-band rejection, and integration.

References

[1] W. J. Choi, *et al.*, "Circuit Implications of MIMO Technology for Advanced Wireless Local Area Networks," 200 IEEE RFIC Symp. Dig., June 2006.

[2] C.-C. Lin, *et al.*, "Single-chip dual-band WLAN power amplifier using InGaP/GaAs HBT," 2005 IEEE European Microwave Symp. Dig., Oct. 2005.

[3] Hsin-Hsing Liao, *et al.,* " A fully integrated 2×2 power amplifier for dual band MIMO 802.11n WLAN application using SiGe HBT technology," 2008 IEEE RFIC Symp. Dig., June 2008.

[4] Ali Afsahi1, *et al.*, "Fully Integrated Dual-Band Power Amplifiers with on-chip Baluns in 65nm CMOS for an 802.11n MIMO WLAN SoC," 2009 IEEE RFIC Symp. Dig., June 2009.

[5] C.-W. P. Huang, *et al.*, " Innovative Architecture for Dual-band WLAN and MIMO Front-end Module Based on a Single Pole, Three Throw Switch-plexer," 2009 IEEE RFIC Symp. Dig., June 2009.

[6] Gregory Yuen, *et al.*, "Dual Signal RF Power Level Detector," International Patent Application No. PCT/CA2004/001404.